

Novel 3-Oxa Lipoxin A₄ Analogues with Enhanced Chemical and Metabolic Stability Have Anti-inflammatory Activity in Vivo

William J. Guilford,^{*,†} John G. Bauman,[†] Werner Skuballa,[‡] Shawn Bauer,[†] Guo Ping Wei,[†] David Davey,[†] Caralee Schaefer,[§] Cornell Mallari,[§] Jennifer Terkelsen,[§] Jih-Lie Tseng,[#] Jun Shen,[#] Babu Subramanyam,[#] Arndt J. Schottelius,^{||} and John F. Parkinson[⊥]

Departments of Medicinal Chemistry, Immunology, Animal Pharmacology, and Pharmacokinetics and Drug Metabolism, Berlex Biosciences, 2600 Hilltop Drive, Richmond, California 94804, and Research Business Area Dermatology and Medicinal Chemistry, Schering AG, Berlin, Germany

Received November 11, 2003

Lipoxin A₄ (LXA₄) is a structurally and functionally distinct natural product called an eicosanoid, which displays immunomodulatory and anti-inflammatory activity but is rapidly metabolized to inactive catabolites in vivo. A previously described analogue of LXA₄, methyl (5*R*,6*R*,7*E*,9*E*,11*Z*,13*E*,15*S*)-16-(4-fluorophenoxy)-5,6,15-trihydroxy-7,9,11,13-hexadecatetraenoate (**2**, ATLa), was shown to have a poor pharmacokinetic profile after both oral and intravenous administration, as well as sensitivity to acid and light. The chemical stability of the corresponding *E,E*-trien-11-yne analogue, **3**, was improved over **2** without loss of efficacy in the mouse air pouch model of inflammation. Careful analysis of the plasma samples from the pharmacokinetic assays for both **2** and **3** identified a previously undetected metabolite, which is consistent with metabolism by β -oxidation. The formation of the oxidative metabolites was eliminated with the corresponding 3-oxatetraene, **4**, and the 3-oxatrien-11-yne, **5**, analogues of **2**. Evaluation of 3-oxa analogues **4** and **5** in calcium ionophore-induced acute skin inflammation model demonstrated similar topical potency and efficacy compared to **2**. The 3-oxatrien-11-yne analogue, **5**, is equipotent to **2** in an animal model of inflammation but has enhanced metabolic and chemical stability and a greatly improved pharmacokinetic profile.

Introduction

Lipoxins are a structurally and functionally distinct class of natural products called eicosanoids, which play a key role in inflammation. Arachidonate-derived lipid mediators such as prostaglandins or leukotrienes are involved in the initiation and maintenance of inflammatory responses and are proinflammatory; however, lipoxins are involved in the regulation and resolution of inflammation and are anti-inflammatory.¹ Since lipoxin A₄ (**1**, LXA₄, Figure 1) was reported in 1984,² the trihydroxytetraene structure has attracted the attention of synthetic chemists, as seen in a number of reported syntheses.^{3–6} The potent anti-inflammatory and immunomodulatory activity of LXA₄ has attracted the attention of researchers for use as a treatment of allergic asthma,⁷ T cell-mediated dermatoses, and inflammatory bowel diseases and as a gastroprotective agent.⁸ Development of LXA₄, however, has been limited by its metabolic and chemical instability.

The metabolic instability of the natural product, LXA₄, is the result of a series of steps initiated by the rapid oxidation of the 15(*S*) alcohol by prostaglandin dehydrogenase (PGDH) to form inactive catabolites, as 15-oxo-LXA₄ and 13,14-dihydro-LXA₄.⁹ The initial de-

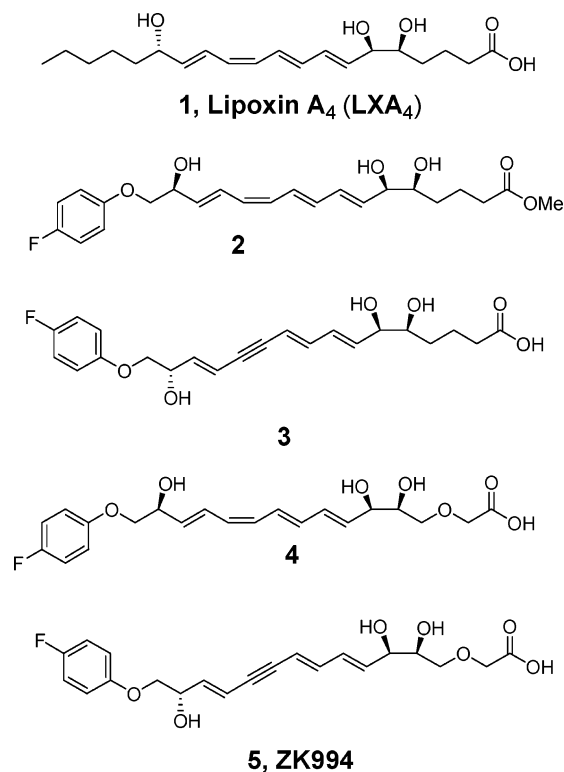


Figure 1. Lipoxin A₄ and analogues.

sign of metabolically stable LXA₄ analogues focused on identifying poor substrates for PGDH,¹⁰ which maintained potency in in vitro assays. The discovery that 15-epi-LXA₄, or aspirin-triggered LXA₄, was equipotent in

* To whom correspondence should be addressed. Phone: 510 669 4065. Fax: 510 669 4310. E-mail: william_guilford@berlex.com.

[†] Department of Medicinal Chemistry, Berlex Biosciences.

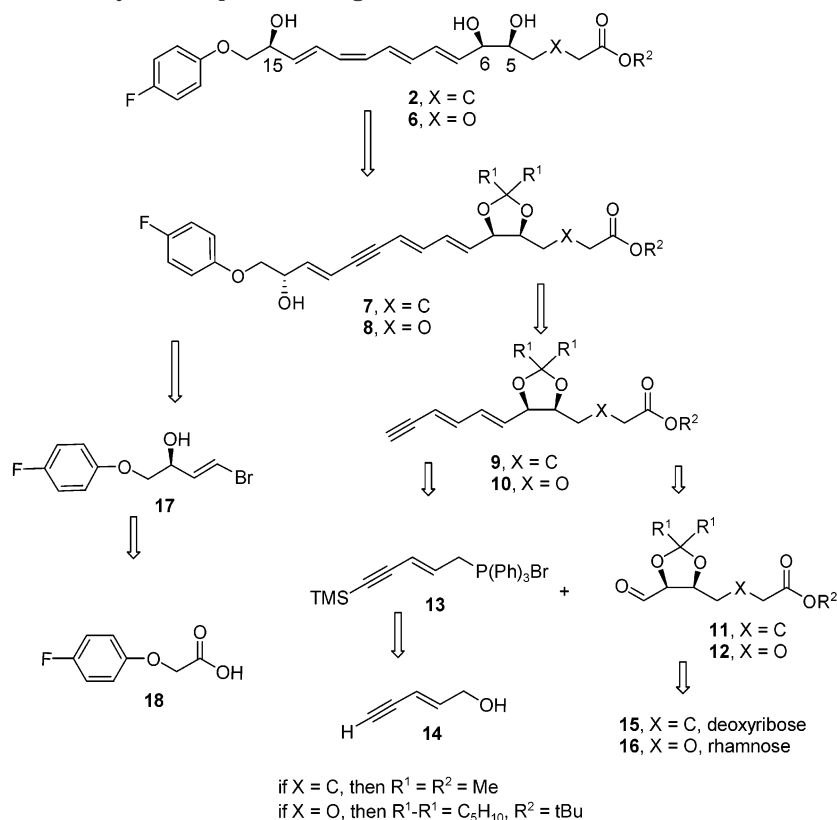
[‡] Medicinal Chemistry, Schering AG.

[§] Department of Animal Pharmacology, Berlex Biosciences.

[#] Department of Pharmacokinetics and Drug Metabolism, Berlex Biosciences.

^{||} Research Business Area Dermatology, Schering AG.

[⊥] Department of Immunology, Berlex Biosciences.

Scheme 1. Retrosynthetic Analysis of Lipoxin Analogues

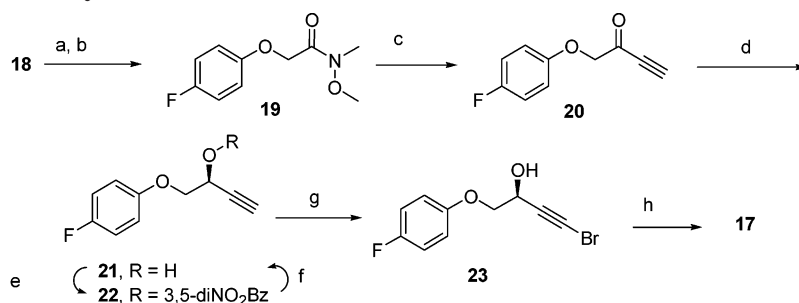
in vitro assays to LXA₄ but was a poorer substrate for PGDH provided support for the potential novel analogue design. Several structural elements were combined in **2**, methyl (5*R*,6*R*,7*E*,9*E*,11*Z*,13*E*,15*S*)-16-(4-fluorophenoxy)-5,6,15-trihydroxy-7,9,11,13-hexadecatetraenoate (15-epi-16-(*p*-fluoro)phenoxy-LXA₄, ATLa, ATLa2), which has enhanced metabolic stability and was selected for scale-up and further testing. The potent anti-inflammatory and immunomodulatory properties of **2** were demonstrated in a series of in vivo models, including an allergic airway inflammation model,¹¹ a T-cell-dependent skin inflammation model,¹² a dextran sulfate (DSS) induced colitis model,¹³ and an adaptive immunity model with 5-LO knockout mice.¹⁴ Taken together, these studies provide evidence that **2** can directly or indirectly modulate T cell effector function in the setting of Th₁- and Th₂-dependent inflammation and adaptive immunity.

Although **2** has enhanced metabolic stability over LXA₄ in vivo, **2** is reported to be cleared within 15 min after intravenous injection in the mouse.¹⁵ In addition, **2** shares the same trihydroxytetraene structure with LXA₄ and, therefore, has the same chemical stability issues, light and acid sensitivity. LXA₄ isomerizes to a mixture of double bond isomers including the corresponding *E,E,E,E*- or 11-*trans*-LXA₄ in the presence of light and decomposes to a mixture of products in the presence of strong acid. To circumvent the metabolic and chemical stability issues, we explored simple replacements for the *E,E,Z,E*-tetraene unit that would maintain potency. Herein, we describe the results of our effort to identify analogues of **2** that have increased metabolic and chemical stability, improved pharmacokinetics, and anti-inflammatory activity in vivo, which led to the discovery of **5**.

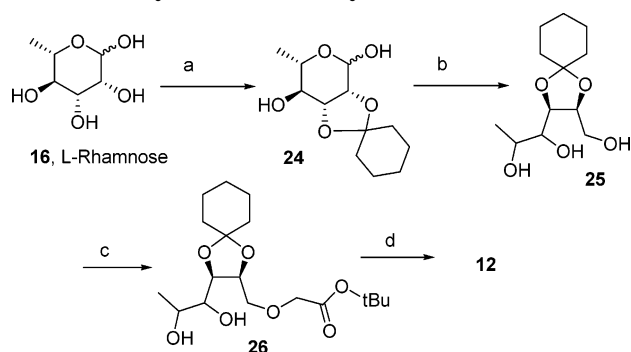
Chemistry

The structure of **2** and **3** can be characterized as a linear chain of 16 carbons in which all but three carbon atoms are either unsaturated or substituted with oxygen. The 3-oxa analogues **4** and **5** differ in that all of the carbon atoms in the chain are either unsaturated or substituted with oxygen. As in the reported synthesis of **2**,¹⁶ the retrosynthetic analysis of the lipoxin analogues is based on the Nicolaou synthesis of lipoxin A₄ (**1**) and is shown in Scheme 1.¹⁷ This convergent approach divides the molecule into three parts: an enyne Wittig reagent (**13**),¹⁸ an aldehyde (**11** or **12**), and a vinyl bromide unit (**17**). The stereochemistry at C5 and C6 is set with the starting sugar, **15** or **16**, and the stereochemistry at C15 is set by a chiral reduction. The geometry of the C9–C10 double bond is established with starting *E*-pentenynol, **14**. The geometry of the C13–C14 double bond is set by reduction of an acetylenic alcohol (Scheme 2). The geometry of the C7–C8 and C11–C12 double bonds is set during the synthesis.

Preparation of the vinyl bromide intermediate is shown in Scheme 2. Weinreb amide **19** was prepared from 4-fluorophenoxyacetic acid, **18**, through the corresponding acid chloride. Treatment of amide **19** with lithium acetylide gave ketone **20**, which was reduced with the chiral reducing agent *R*-Alpine-Borane.¹⁹ Although the enantiomeric excess of **21** was typically in the 60–70% range, material having >98% ee was obtained by recrystallization of the corresponding dinitrobenzoyl derivative (**22**). Hydrolysis of the dinitrobenzoyl ester followed by bromination of the acetylene with *N*-bromosuccinimide and silver nitrate gave the acetylenic bromide **23**.²⁰ Reduction of the acetylenic bromide

Scheme 2. Preparation of Vinyl Bromide **17**^a

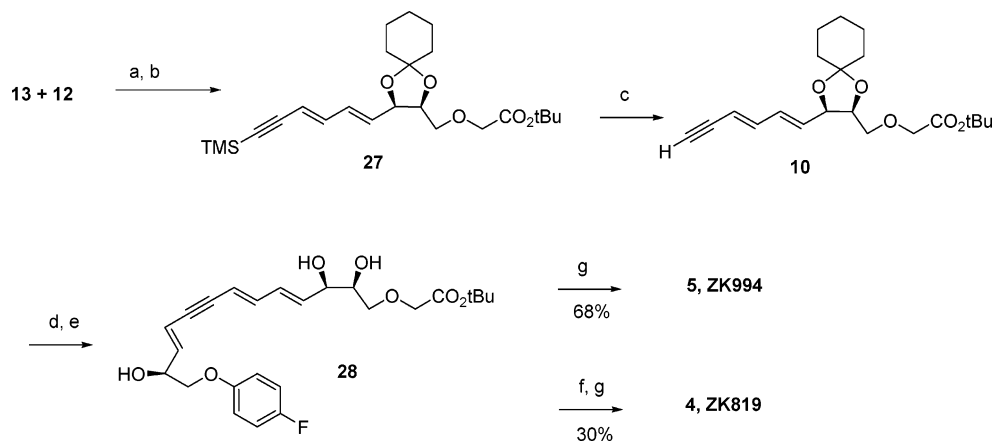
^a (a) (COCl)₂, DMF, ether; (b) MeON(H)Me·HCl, sat. K₂CO_{3(aq)}, EtOAc, 0 °C, 73% from **18**; (c) HCCMgBr, THF, 40 min, 91%; (d) *R*-Alpine-Borane, 97% (e) 3,5-dinitrobenzoyl chloride, TEA, DMAP, CH₂Cl₂, 0 °C, 1–2 h, followed by recrystallization, 54%; (f) K₂CO₃, MeOH, THF, 3.5 h, 80%; (g) NBS, AgNO₃, acetone, 99%; (h) AlCl₃, LiAlH₄, ether, 81%.

Scheme 3. Synthesis of Aldehyde **12** from Rhamnose^a

^a (a) H₂SO₄, Cu(II)SO₄, cyclohexanone, room temp, 16 h, 57%; (b) NaBH₄, MeOH, 3 h, room temp, 88%; (c) toluene, 25% NaOH_(aq), Bu₄N, HSO₄, ^tBu bromoacetate, 44%; (d) H₂O, acetone, NaIO₄, 92%.

with a lithium aluminum hydride/aluminum chloride mixture gave the desired *E*-vinyl bromide **17**.²¹

Lipoxin analogues **2** and **3** were prepared from deoxyribose **15** via dienyne **9** using a procedure described earlier¹⁶ (Scheme 1). Sonogashira coupling of dienyne **9** and vinyl bromide **17** gave the complete carbon skeleton as the trienyne **7**.¹⁷ Hydrolysis of the isopropylidene ketal under acidic conditions and methyl ester under basic conditions gave **3**. The relatively good acid stability of the trien-11-yne unit was demonstrated by the treatment of **7** with 1 N HCl needed to cleave the ketal protecting group in good yield. Treatment of deketalized **7** with activated zinc using the Boland procedure²² gave **2**.

Scheme 4. Synthesis of 3-oxa-lipoxin Analogues^a

^a (a) BuLi, THF, 30–0 °C, 3 h; (b) I₂, CH₂Cl₂, 1 h, 49% from **12**; (c) TBAF, THF, 99%; (d) (Ph₃P)₄, Et₂NH, CuI, THF, **17**, 50%; (e) AcOH, H₂O, EtOAc, 58%; (f) Zn, AgNO₃, Cu(II)(OAc)₂, MeOH, H₂O; (g) NaOH, H₂O, MeOH.

Introduction of the 3-oxa group into the dienyne unit, **10**, was accomplished as outlined in Scheme 3. Cyclohexylidene ketal, **24**, prepared from rhamnose, **16**,²³ was reduced with sodium borohydride to triol **25**. Selective O-alkylation of the primary hydroxyl group using phase-transfer conditions and *tert*-butyl bromoacetate gave ether **26**. The desired aldehyde, **12**, was prepared by oxidative cleavage of **26** using sodium metaperiodate. Coupling of **12** and **13** yielded dienyne, **27**, as a mixture of *E,E* and *E,Z* isomers (Scheme 4). Iodine-catalyzed isomerization to the *E,E*-dienyne **27** and removal of the trimethylsilyl protecting group gave intermediate **10**. Palladium-catalyzed Sonogashira coupling of **10** and **17** followed by hydrolysis of the cyclohexylidene ketal gave the corresponding *tert*-butyl ester **28**. As in the case of esters of **3**, the trienyne unit was stable to acid over a 24 h period required to cleave the ketal. Base-catalyzed ester hydrolysis gave **5**. Reduction of **28** with activated zinc²² gave the *E,E,Z,E*-tetraene and subsequent ester hydrolysis yielded **4**.

Identification of Metabolite

Since the report¹⁵ that **2** is cleared from the mouse within 15 min after intravenous injection, using a dose of 2 μg per mouse, the pharmacokinetic parameters of **2** and related analogues were evaluated in the rat at a dose of 5 mg/kg (about 1 mg per rat). The results are shown in Table 1. Evaluation of the pharmacokinetic parameters of **2** in the rat was complicated by the rapid hydrolysis of the methyl ester in rat plasma to the corresponding carboxylic acid, **29** (see Figure 2). The

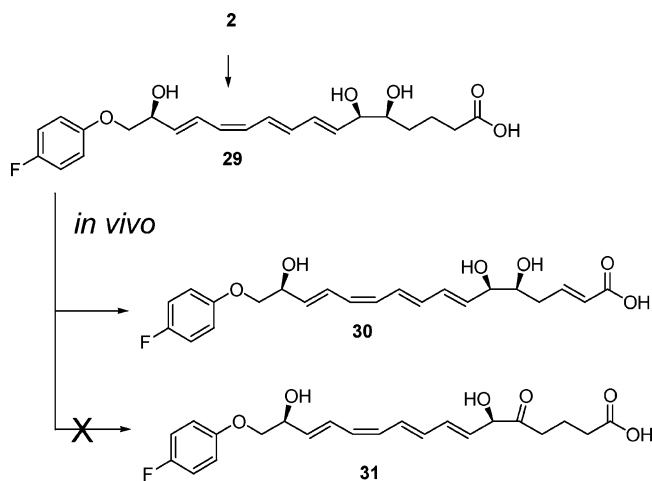


Figure 2. Proposed metabolites of **2**.

Table 1. Pharmacokinetic Data in the Rat after iv ($n = 3$, 3 mg/kg) and po ($n = 3$, 5 mg/kg) Dosing

compd	iv			po			
	$T_{1/2}$, h	Cl, (mL/mg)/kg	AUC _{all} , (h·μg)/mL	$T_{1/2}$, h	C_{max}	T_{max} , h	F , %
2	0.3	51	1.0	0.5	0.2	0.5	12
29	0.2	28	1.8	1.1	0.3	1.0	13
3	0.1	58	0.9	1.8	0.2	0.5	28
4	1.3	50	1.0	1.1	0.04	0.5	4
5	2.3	7	7.0	2.2	0.4	1.3	14

calculated pharmacokinetic parameters for **2** listed in Table 1 were obtained by dosing **2** but analyzing the plasma samples for **29**. The half-life of **2** and **29** were about 15 min, in agreement with the data reported in mice.¹⁵ Careful analysis of the plasma samples indicated the presence of a metabolite, which had a molecular weight 2 mass units lower than that of **29**. Since compound **2** was designed to minimize all the known major metabolic routes, the identification of a new metabolite by LC/MS–MS was unexpected. The UV spectra of both **29** and the metabolite were identical, which is consistent with an intact *E,E,Z,E*-tetraene chromophore⁹ and minimal structural modification. Two structures were consistent with the data: **30** and **31** (see Figure 2). Since the metabolite was stable to treatment with sodium borodeuteride in methanol, the 5-oxo structure, **31**, could be ruled out and the structure of the metabolite was assigned as the 2,3-dehydro analogue **30**. Attempts to isolate **30** from in vitro metabolism studies, such as liver microsomes, for a more complete structural determination were unsuccessful. By analogy to lipid metabolism in the prostaglandin^{24,25} and leukotriene²⁶ fields, we propose that **30** would be formed as the first step in the β -oxidation of **2**. Consistent with the proposal, the corresponding 2-mass-unit-lower metabolite was observed during a pharmacokinetic assay of **3** in rats but not in 3-oxa analogues **4** and **5**, which were designed to eliminate this pathway.²⁷

The pharmacokinetic parameters for tetraene analogue **2** is characterized by rapid clearance and relatively short half-lives after both oral gavage (po) and intravenous injection (iv). The corresponding trienylene analogue, **3**, had similar properties after iv administration but a significantly better effective half-life after oral administration. The elimination of the β -oxidation pathway had a minimal impact on the pharmacokinetic profile

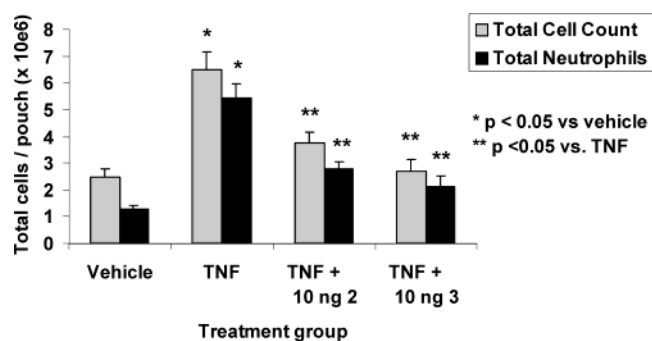


Figure 3. Tetraene and trienylene lipoxin analogues are both anti-inflammatory in vivo. Analogues **2** and **3** were tested for local anti-inflammatory effects in the murine dorsal air pouch model of TNF-induced inflammation, as described in “Experimental Section” and ref 29. The figure shows the effect of 10 ng of locally delivered analogues on total leukocyte (grey bars) and neutrophil (black bars) cell counts in the pouch exudate 4 h following TNF administration. A robust and similar inhibitory effect (~50%) on TNF-induced leukocyte trafficking into the pouch was observed for **2** and **3**. Data are the mean \pm SEM from $N = 20$ mice: (*) $p < 0.05$ versus vehicle; (**) $p < 0.05$ versus TNF.

of **4** compared with **2**, **29**, or **3**. In contrast, trienylene **5** had a significantly improved half-life and a significantly reduced clearance after both po and iv dosing in the rat. The similar F values in the rat for **2** and **5** hide the improved pharmacokinetic parameters of **5** as determined by the area under the curve value, AUC_{all} after iv dosing. Comparison of the corresponding pharmacokinetic parameters for **2** and **5** in the dog after iv dosing (2 mg/kg) are complicated by the incomplete ester hydrolysis of **2**. Comparison of the pharmacokinetic parameters for **5** in the dog versus the rat shows a slight increase in the iv half-life from 2.3 to 2.7 h (2 mg/kg) and a slight increase in the po half-life from 2.2 to 3.2 h (2 mg/kg). Similar improvements in C_{max} and T_{max} values after oral dosing increased the F value for **5** in the dog to 40.

In Vivo Models of Inflammation. Analogue **2** has been shown to be efficacious in the TNF α -induced murine dorsal air pouch model, which is an acute experimental model of inflammation.^{28–30} The model is characterized by cellular infiltration into a localized area, i.e., air pouches raised on the dorsal area of mice. Once the air pouch is established and stabilized, an injection of TNF α induces a temporal infiltration of inflammatory cells into the air pouch. The infiltrate is predominantly composed of proinflammatory neutrophils but also contains eosinophils and smaller numbers of mononuclear cells (monocytes and T- and B-lymphocytes). Four hours after injection of the compound and TNF α , the cells were harvested from the air pouch for enumeration and differential count analysis. As seen in Figure 3, compounds **2** and **3** showed a significant decrease in the total number of cells and neutrophils infiltrating into the air pouches at similar doses of 10 ng/pouch compared with vehicle-treated mice.

Topical efficacy for native LXA₄, **1**, and **2** has been demonstrated in several models of skin inflammation.¹² The calcium ionophore model was chosen to compare 3-oxa analogues **4** and **5** with **2**. In this model, calcium ionophore A-23187 with or without anti-inflammatory agents is applied topically to the ears of a mouse, which induces acute inflammation with edema and granulo-

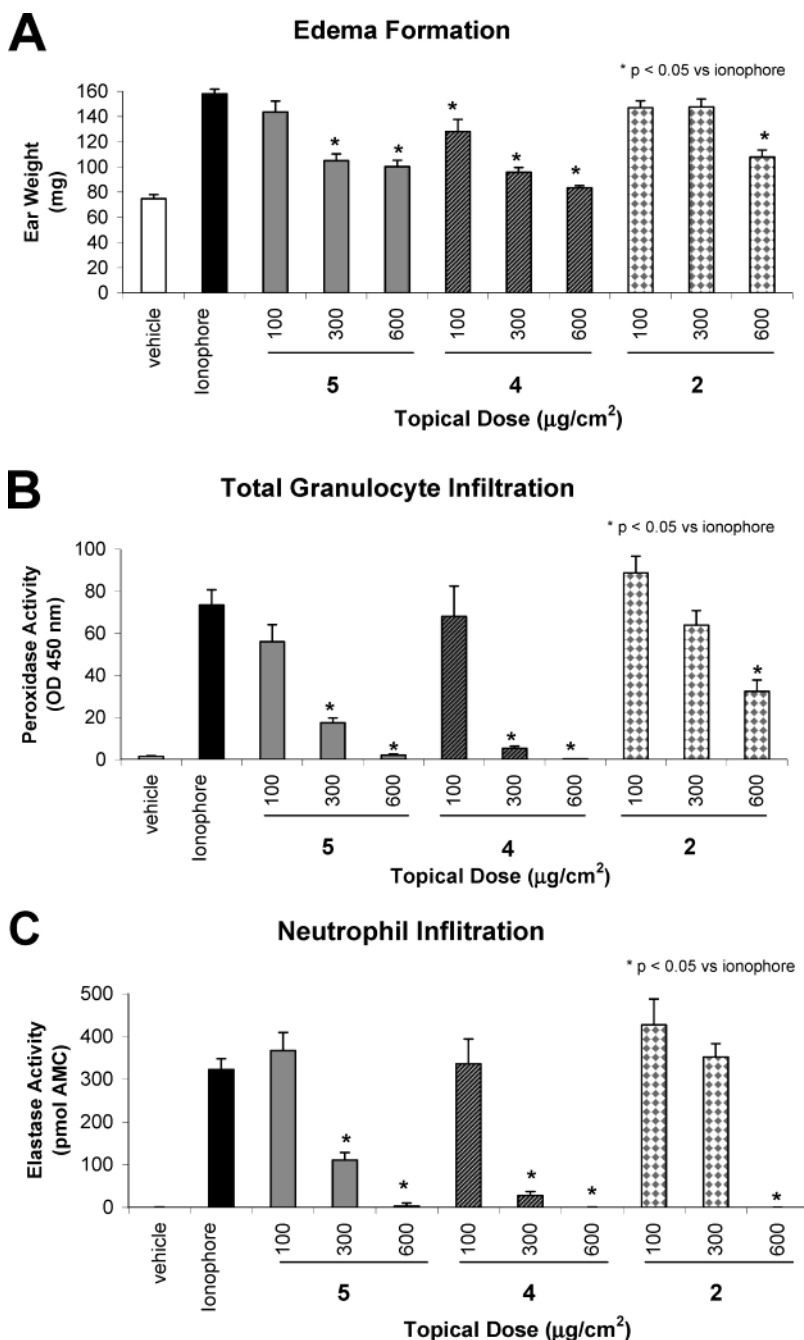


Figure 4. 3-Oxa-lipoxin analogues are potent topical anti-inflammatory agents. Acute mouse ear skin inflammation was induced by topical application of 0.1% w/v calcium ionophore in isopropylmyristate, as described in “Experimental Section” and ref 12. Inflammation was measured after 24 h. Data for vehicle control (open bars), ionophore control (black bars), and treatment by topical coapplication of **5** (gray bars), **4** (gray hashed bars), and the positive control **2** (stippled bars) are shown at doses of 100, 300, and 600 µg/cm². Dose-dependent anti-inflammatory effects were observed on edema (ear weight, panel A), total leukocyte infiltration (peroxidase activity, panel B), and neutrophil infiltration (elastase activity, panel C). ED₅₀ was <300 µg/cm² for **5** and **4** on all endpoints. Data are the mean ± SEM with *N* = 8–to 10 mice for all groups, except *N* = 5 for 600 µg/cm² dose of **2**: (*) *p* < 0.05 versus ionophore control.

cyte infiltration that peaks at approximately 24 h. The extent of granulocyte infiltration was determined using the peroxidase assay. Elastase activity was used as a measure of neutrophil infiltration. Anti-inflammatory effects of a given compound were defined as inhibition of edema formation (Figure 4A), peroxidase activity (Figure 4B), and elastase activity (Figure 4C). The data shown in Figure 4 clearly show that **2**, **4**, and **5** inhibited edema formation and neutrophil and granulocyte infiltration in a dose-dependent manner. In addition, neutrophil and granulocyte infiltration was completely

inhibited at the highest dose tested (600 µg/cm²). The IC₅₀ for **4** and **5** on all three topical efficacy parameters was <300 µg/cm².

Conclusion

The natural product, lipoxin A₄, has immunomodulatory and anti-inflammatory activity but is rapidly metabolized to inactive catabolites in vivo. Chemically and metabolically stable LXA₄ analogues of **2**, which are equipotent in animal models of inflammation, have been reported. The synthesis of the trienylene and tetraene

analogues is described in both the carbon and 3-oxa series. In the carbon series, we demonstrated that the tetraene unit is not needed for efficacy in the air pouch model of inflammation. On the basis of the identification of a new metabolic route for **2**, the β -oxidation-resistant 3-oxa series was developed (trienyne, **5**, and tetraene, **4**) with anti-inflammatory activity comparable to that of **2** in cutaneous inflammation. On the basis of the increased acid, metabolic, and UV stability, equivalent anti-inflammatory activity, improved pharmacokinetic parameters, and ease of synthesis, **5** has pharmaceutical properties suitable for clinical development. Taken together, the results provide new insights on the in vivo catabolism of lipoxins and structure–activity relationships essential for in vivo actions. The 3-oxa-based lipoxin A₄ analogues provide superior pharmacophores with which to explore preclinical and clinical concepts in immunomodulation.

Experimental Section

All starting materials not described below were purchased from commercial sources. All reagents and solvents were used as received from commercial sources without additional purification. Elemental analyses were performed by Robertson Microlit Laboratories (Madison, NJ), and results were within $\pm 0.4\%$ of the calculated values. Proton NMR spectra were recorded with a Varian XL-300 spectrometer at 400 MHz proton and were consistent with the assigned structures. Carbon-13 NMR spectra at 100 and 125 MHz were obtained on a Varian XL-300 spectrometer and the Bruker Avance 500 spectrometer. HPLC was performed with a Rainin SD-1 Dynamax system and a C-18 reverse-phase Dynamax 60A column using a gradient of methanol (0.1% TFA) or acetonitrile (0.1% TFA) in water (0.1% TFA). The enantiomeric excess of **21** was determined by HPLC analysis on the corresponding dinitrobenzoate, **22**, using a Diacel Chiralpak AD (4.6 mm \times 250 mm, 60% 2-propanol/hexane, 1 mL/min), which separates the (*R*) (11.5 min) and the (*S*) (19.3 min) enantiomers.

Identification of the Metabolite of 2. Since **2** is rapidly metabolized in plasma to the corresponding acid **29**, the standard analytical protocol for analysis of **2** in biological samples was developed for **29**. Analytical quantification was carried out using LXA₄ as an internal standard using a C18 column (Waters XTerra RP18, 5 μ m, 2.1 mm \times 50 mm) and a 10–80% “A” in “B” gradient over 2 min (6 min total run time). Solvent “A” was water with 0.1% formic acid, and solvent “B” was acetonitrile with 0.1% formic acid. The MS–MS method monitored the *m/e* = 403–111 (negative ionization conditions).

***N*-Methoxy-*N*-methyl-2-(4-fluorophenoxy)ethanamide (19).** Oxalyl chloride (60 mL, 686 mmol) and a catalytic amount of dimethylformamide were added to a stirred suspension of 2-(4-fluorophenoxy)ethanoic acid (**18**, 97.3 g, 572 mmol) in dichloromethane (500 mL). After 22 h, the mixture was concentrated under vacuum to obtain 108 g of the corresponding acid chloride as a yellow oil in quantitative yield: ¹H NMR (CDCl₃) δ 4.90 (s, 2H), 6.84 (m, 2H), 6.99 (m, 2H) ppm. The residue was added slowly to a stirred suspension of *N,O*-dimethylhydroxylamine hydrochloride (55.80 g, 572 mmol) in saturated potassium carbonate and ethyl acetate (375 mL). A moderately exothermic reaction occurred. After 20 min, the reaction mixture was partitioned between water and ether. The ether layer was washed with 1 M hydrochloric acid and saturated sodium chloride, dried over magnesium sulfate, and concentrated under vacuum to give **19** as an off-white crystalline solid, 113.05 g (73% yield from starting acid): ¹H NMR (CDCl₃, 400 MHz) δ 3.21 (s, 3H), 3.73 (s, 3H), 4.75 (s, 2H), 6.87 (m, 2H), 6.95 (m, 2H) ppm.

4-(4-Fluorophenoxy)-1-butyne-3-one (20). A solution of **19** (20.00 g, 74 mmol) in THF (100 mL) was cooled in an ice bath as a solution of ethynylmagnesium bromide (0.5 M in THF, 508 mL, 254 mmol) was added. After an additional 30 min at 0 °C, the reaction mixture was poured into a vigorously stirred mixture of 1 M NaHSO₄ (1700 mL) and ether (1 L). The layers were separated, and the aqueous layer was then extracted with ether (700 mL). The combined organic phases were washed with brine and dried over MgSO₄, filtered, and concentrated under vacuum. The residue was purified by eluting through a plug of silica gel (10 cm \times 3 cm) with 1:4 ether/petroleum ether to afford 27.65 g (91% yield) as a low-melting solid: ¹H NMR (CDCl₃) δ 3.40 (s, 1H), 4.70 (s, 2H), 6.85 (m, 2H), 7.0 (t, 2H) ppm.

(3*S*)-4-(4-Fluorophenoxy)-3-hydroxy-1-butyne (21). A solution of *R*-Alpine-Borane (0.5 M in THF, 930 mL, 465 mmol) was evaporated to dryness under vacuum to give about 150 g of a thick syrup. Neat **20** (27.6 g, 155 mmol) was added, and the reaction mixture was stirred for 2 days. The reaction mixture was cooled to 0 °C, and acetaldehyde (26 mL, 465 mmol) was added to quench the excess reagent. After being stirred at ambient temperature for 2 h, the reaction mixture was placed under vacuum and stirred first at 0 °C for 1 h, then at 65 °C for 2 h. The reaction mixture was cooled to ambient temperature, and ether (300 mL) was added under nitrogen. Ethanolamine (30 mL, 465 mmol) was added dropwise at 0 °C, and the resulting reaction mixture was stored in the freezer overnight. The resulting precipitate was removed by filtration and washed with cold ether. The combined filtrates were concentrated under vacuum. Purification by flash chromatography on a 2.5 L column using a 10–25% gradient of ethyl acetate in hexane gave 27 g (97%): ¹H NMR (CDCl₃) δ 2.56 (s, 1H), 4.10 (m, 2H), 4.78 (m, 1H), 6.85 (m, 2H), 7.0 (m, 2H). This material was determined to be about 64% ee based on chiral HPLC of its 3,5-dinitrobenzoyl ester. To a solution of **21** (about 490 mmol) in methylene chloride (1 L) was added, between –5 and 0 °C, 3,5-dinitrobenzoyl chloride (125 g, 539 mmol), followed by slow addition of triethylamine (10.8 mL, 77 mmol) and a catalytic amount of (dimethylamino)pyridine (20 mg). After being stirred for 40 min, the reaction mixture was cautiously partitioned between methylene chloride and aqueous sodium bicarbonate. The aqueous layer was extracted with dichloromethane. The combined organic layers were washed with water and brine, dried over Na₂SO₄, filtered through a pad of silica gel, and concentrated to give a tan solid. Rapid recrystallization from a 99:1 mixture of methanol/acetic acid (5 L) gave 101 g (54%) of the enantiomerically enriched product as fluffy white needles. This material was determined to have >98% ee by HPLC: ¹H NMR (CDCl₃) δ 2.65 (s, 1H), 4.40 (m, 2H), 6.05 (m, 1H), 6.90 (m, 2H), 7.0 (t, 2H), 9.15 (s, 2H), 9.25 (s, 1H) ppm. To a solution of **22** (10.35 g, 98% ee, 27.6 mmol) in THF (115 mL), was added methanol (115 mL) and potassium carbonate (0.58 g). After being stirred for 3.5 h, the reaction mixture was quenched with acetic acid (2 mL). The solvents were evaporated. The resulting slurry was filtered, and the solid was washed with ether. The filtrate was concentrated, and the filtration/ether wash sequence was repeated to give 4.02 g (80%): ¹H NMR (CDCl₃) δ 2.56 (s, 1H), 4.10 (m, 2H), 4.78 (m, 1H), 6.85 (m, 2H), 7.0 (m, 2H).

(3*S*)-1-Bromo-4-(4-fluorophenoxy)-3-hydroxy-1-butyne (23). A mixture of **21** (2.5 g, 14 mmol), *N*-bromosuccinimide (2.74 g, 15.4 mmol), and silver nitrate (0.12 g, 0.7 mmol) in acetone (70 mL) was stirred at ambient temperature. The pale solution became cloudy over 30 min. The mixture was concentrated. Filtration through a plug of silica gel, eluting with 20% ethyl acetate in hexane, gave 3.6 g (99%) of a pale-yellow oil: ¹H NMR (CDCl₃) δ 3.95–4.15 (m, 2H), 4.75 (m, 1H), 6.86 (m, 2H), 6.97 (m, 2H) ppm.

(1*E*,3*S*)-1-Bromo-4-(4-fluorophenoxy)-3-hydroxy-1-butene (17). Aluminum chloride (2.79 g, 21 mmol) was added in portions to a mixture of lithium aluminum hydride (1.06 g, 28 mmol) in ether (70 mL). A solution of **23** (3.6 g) in ether (10 mL) was added cautiously. A vigorous reaction with evolution of hydrogen gas was observed. The mixture was

warmed to reflux in a water bath for 30 min. The reaction mixture was cooled to 0 °C and treated sequentially with 2.8 mL of water, 2.8 mL of 15% NaOH, and 8.4 mL of water. The resulting suspension was stirred for 10 min and filtered, and the solids were washed with THF and ether. The filtrate was concentrated to afford 2.94 g (81%): ¹H NMR (CDCl₃) δ 2.41 (t, 1H), 3.85 (dd, 1H), 3.99 (dd, 1H), 4.50 (m, 1H), 6.31 (dd, 1H), 6.52 (dd, 1H), 6.83 (m, 2H), 6.97 (t, 2H) ppm.

(2*R*,3*R*)-3-(1,2-Dihydroxypropyl)-1,4-dioxaspiro[4,5]-decane-2-carboxaldehyde (24). Rhamnose hydrate (100 g, 0.55 mol) was converted into 92.3 g (0.31 mol, 57%) of cyclohexylidene ketal as described earlier:²³ [α]_D +0.46 (10.49 mg/cc, MeOH); ¹H NMR (CDCl₃) δ 1.34 (d, 3H), 1.40 (m, 2H), 1.6 (m, 8H), 2.78 (d, 1H), 3.0 (s, 1H), 3.9 (m, 1H), 4.07 (m, 1H), 4.6 (d, 1H), 4.9 (m, 1H), 5.4 (s, 1H) ppm. Anal. (C₁₂H₂₀O₅·0.5C₆H₁₀O) C, H.

(2*R*,3*S*)-α²-(1-Hydroxyethyl)-1,4-dioxaspiro[4,5]decane-2,3-dimethanol (25). A slurry of sodium borohydride (34.2 g, 0.9 mol) in methanol (400 mL) was cooled in an ice bath and treated with a solution of **24** (92 g, 0.27 mol) in methanol (200 mL). The reaction mixture was stirred for about 4 h before the addition of acetic acid to adjust the pH to about 6 (about 120 mL). The reaction mixture was filtered. The filtrate was concentrated to give a slightly yellow viscous oil. Treatment of an ether solution with hexane gave 81.2 g (88%) of an off-white solid after drying: ¹H NMR (CD₃OD) δ 1.28 (d, 3H), 1.43 (m, 2H), 1.7 (m, 8H), 3.42 (dd, 1H), 3.7 (m, 3H), 4.25 (m, 1H), 4.42 (dd, 1H) ppm.

1,1-Dimethylethyl [(2*S*,3*R*)-3-(1,3-Dihydroxypropyl)-1,4-dioxaspiro[4,5]dec-2-yl]methoxy]acetate (26). A mixture of **25** (81 g, 0.32 mol) and *tert*-butyl bromoacetate (77 g, 0.39 mol, 1.2 equiv) in 1 L of toluene and 80 mL of aqueous sodium hydroxide (25 wt %) was stirred as tetrabutylammonium sulfate (7.8 g, 23 mmol, 0.07 equiv) was added. After about 16 h, the reaction mixture was diluted with ethyl acetate and saturated aqueous monobasic potassium phosphate. The combined organic layers were dried and concentrated to give a clear oil. Purification on silica gel using a step gradient of ether in hexane (20–50%) gave 50.8 g (44%) of an oil: [α]_D +8.59 (10.30 mg/cc, MeOH); ¹H NMR (CDCl₃) δ 1.24 (d, 3H), 1.35 (m, 2H), 1.47 (s, 9H), 1.6 (m, 8H), 3.6 (m, 2H), 3.8 (m, 2H), 3.95 (m, 2H), 4.32 (m, 1H), 4.4 (m, 1H) ppm. Anal. (C₁₈H₃₂O₇·0.2H₂O) C, H.

1,1-Dimethylethyl [(2*S*,3*S*)-3-Formyl-1,4-dioxaspiro[4,5]dec-2-yl]methoxy]acetate (12). A solution of **26** (50 g, 138 mmol) in acetone (350 mL) was treated with a solution of periodate (50 g, 235 mmol, 1.7 equiv) in water (1.2 L). After about 4 h, solvent was removed by distillation and the residue was extracted with ethyl acetate (3 × 500 mL). The combined organic layers were dried and concentrated under reduced pressure without heating to give 40 g (92%) of a clear oil: [α]_D -1.14 (10.15 mg/cc, MeOH); ¹H NMR (CDCl₃) δ 1.38 (m, 2H), 1.42 (s, 9H), 1.61 (m, 8H), 1.73 (m, 2H), 3.52 (dd, 1H), 3.72 (dd, 1H), 3.88 (s, 2H), 4.38 (dd, 1H), 4.52 (m, 1H), 9.62 (s, 1H) ppm. Anal. (C₁₆H₂₆O₆) C, H.

1,1-Dimethylethyl [(2*S*,3*R*)-3-[(1*E*,3*E*)-6-(Trimethylsilyl)-1,3-hexadien-5-ynyl]-1,4-dioxaspiro[4,5]dec-2-yl]methoxy]ethanoate (27). A slurry of phosphonium salt (**13**, 67.1 g, 0.14 mol) in THF (875 mL) was stirred under nitrogen, cooled in a dry ice acetonitrile bath (-30 °C internal), and treated with a solution of ⁿBuLi (66.5 mL, 0.133 mol, 2 M in hexane) via dropwise addition. The reaction mixture was allowed to warm to about 0 °C, then cooled back to about -30 °C. The reaction mixture was treated with a solution of **12** (40 g, 0.127 mol) in 125 mL of THF. After 1 h, the reaction was diluted with saturated potassium phosphate (pH 5). The aqueous layer was washed with ether (3×). The combined organic layers were washed with water and brine, dried, and concentrated. Impurities were precipitated from an ether solution with hexane. The concentration of the filtrate gave 50.29 g of a 2:1 mixture of *E,Z* to *E,E* isomers by NMR analysis. *Z,E* isomer: ¹H NMR (CDCl₃) δ 0.15 (s, 9H), 1.3 (m, 2H), 1.4 (s, 9H), 1.6 (m, 8H), 3.45 (m, 2H), 3.92 (m, 2H), 4.34

(m, 1H), 5.02 (m, 1H), 5.48 (dd, 1H), 5.6 (d, 1H), 6.16 (dd, 1H), 6.82 (dd, 1H) ppm. The residue was dissolved in methylene chloride (400 mL) and was treated with iodine until a red color persisted. After about 1 h, the reaction mixture was treated with an aqueous solution of sodium hydrosulfite, dried, filtered, and concentrated. Purification by chromatography on silica gel using a gradient of ether in hexane gave 27.8 g (49%) of the desired product: [α]_D -19.10 (10.88 mg/cc, MeOH); ¹H NMR (CDCl₃) δ 0.15 (s, 9H), 1.3 (m, 2H), 1.4 (s, 9H), 1.6 (m, 8H), 3.45 (m, 2H), 3.92 (m, 2H), 4.34 (m, 1H), 4.62 (m, 1H), 5.54 (d, 1H), 5.72 (dd, 1H), 6.26 (dd, 1H), 6.56 (dd, 1H) ppm. Anal. (C₂₄H₃₈SiO₅·0.4H₂O) C, H.

1,1-Dimethylethyl [(2*S*,3*R*)-3-[(1*E*,3*E*)-1,3-Hexadien-5-ynyl]-1,4-dioxaspiro[4,5]dec-2-yl]methoxy]ethanoate (10). A solution of **27** (27.8 g, 63 mmol) in THF (25 mL) was cooled in an ice bath and treated with a solution of tetrabutylammonium fluoride in THF (71 mL, 71 mmol, 1 M in THF). After about 1 h, the reaction mixture was diluted with saturated aqueous monobasic potassium phosphate and ether. The aqueous layer was washed with ether (2×). The combined organic layers were washed with saturated aqueous monobasic potassium phosphate solution and brine solution, dried, and concentrated to give 23.4 g (99%) of an oil: ¹H NMR (CDCl₃) δ 1.3 (m, 2H), 1.4 (s, 9H), 1.6 (m, 8H), 3.02 (s, 1H), 3.5 (m, 2H), 3.96 (m, 2H), 4.38 (q, 1H), 4.66 (t, 1H), 5.54 (dd, 1H), 5.78 (dd, 1H), 6.33 (dd, 1H), 6.65 (dd, 1H) ppm.

1,1-Dimethylethyl [(2*S*,3*R*)-3-[(1*E*,3*E*,7*E*,9*S*)-10-(4-Fluorophenoxy)-9-hydroxyl-1,3,7-decatrien-5-ynyl]-1,4-dioxaspiro[4,5]dec-2-yl]methoxy]ethanoate (8). A solution of **17** (16.6 g, 63 mmol), solid tetrakis(triphenyl)phosphine-Pd(0) (3.67 g, 3 mmol), and Cu(I) iodide (1.2 g, 6.3 mmol) in diethylamine (50 mL) and THF (800 mL) was stirred and deoxygenated by bubbling argon through the mixture for 90 min. An argon deoxygenated solution of **10** (23 g, 63 mmol) in 200 mL of THF was added dropwise. After 2 h, the reaction mixture was diluted with hexane (about 400 mL), treated with silica gel (about 40 g), and filtered. The solid was washed with a 1:1 solution of ether and hexane. The filtrate was concentrated to give 36.8 g of an oil. Purification by chromatography on silica gel using a 15–50% gradient of ether in hexane gave 16.9 g (50%) as an oil: [α]_D -21.17 (10.16 mg/cc, MeOH); ¹H NMR (CDCl₃) δ 1.3 (m, 2H), 1.4 (s, 9H), 1.6 (m, 8H), 2.42 (s, 1H), 3.5 (d, 2H), 3.96 (m, 4H), 4.38 (q, 1H), 4.58 (m, 1H), 4.66 (t, 1H), 5.72 (m, 1H), 5.78 (dd, 1H), 6.03 (m, 1H), 6.16 (dd, 1H), 6.33 (dd, 1H), 6.58 (dd, 1H), 6.88 (m, 4H) ppm. Anal. (C₃₁H₃₉FO₇) C, H, F.

(5*R*,6*R*,7*E*,9*E*,13*E*,15*S*)-16-(4-Fluorophenoxy)-3-oxa-5,6,15-trihydroxy-7,9,13-hexadecatrien-11-ynoic Acid (5). A solution of **8** (1 g, 1.8 mmol) in acetic acid (50 mL) was diluted with ethyl acetate (50 mL) and placed in a 55 °C oil bath for 20 h. The reaction was complete by TLC analysis. Acetic acid and ethyl acetate were removed by distillation under high vacuum. The residue was diluted with water and extracted with ethyl acetate (3×). The combined organic layers were washed with water, saturated aqueous sodium carbonate, water, and brine solution, dried, and concentrated to give 0.9 g of an oil. Chromatography on an HP-20 column, eluting with a gradient of methanol in water, gave 0.5 g (58%) of **28** upon concentration. The combined fractions were treated with 1 N sodium hydroxide solution (2 mL) and concentrated. The reaction was complete by TLC after about 1 h and the mixture was placed on a column of CHP20P resin (75–150 μm, Mitsubishi Chemical Corp.) and eluted using a gradient of methanol in water to give 0.3 g (68%) of the desired product that solidified upon standing: ¹H NMR (CD₃OD) δ 3.63 (m, 1H), 3.67 (m, 2H), 3.86 (dd, *J* = 9.9, 6.7 Hz, 1H), 3.94 (dd, *J* = 9.7, 4.5 Hz, 1H), 4.11 (s, 2H), 4.15 (t, *J* = 6.1, 1H), 4.50 (dd, *J* = 5.4, 1.5 Hz, 1H), 5.76 (dd, *J* = 15.3, 2 Hz, 1H), 5.95 (dd, *J* = 15, 6.6 Hz, 1H), 6.00 (dt, *J* = 17, 2 Hz, 1H), 6.20 (dd, *J* = 15.8, 5.5 Hz, 1H), 6.38 (dd, *J* = 15.8, 10.8 Hz, 1H), 6.60 (dd, *J* = 15.8, 10.8 Hz, 1H), 6.95 (m, 4H) ppm; ¹³C NMR (100 MHz, CD₃OD) δ 69.1, 71.2, 73.2, 73.5, 73.9, 74.7, 90.7, 91.0, 112.2, 112.4, 116.7, 116.9, 116.9, 131.9, 137.1, 142.4, 142.8, 156.5, 158.8, 174.5 ppm. Anal. (C₂₁H₂₃FO₇·0.2H₂O) C, H, F.

(5*R*,6*R*,7*E*,9*E*,11*Z*,13*E*,15*S*)-16-(4-Fluorophenoxy)-3-oxa-5,6,15-trihydroxy-7,9,11,13-hexadecatetraenoic Acid (**4**). Activated zinc was prepared from 10 g of zinc using the Boland procedure.²² A solution of ester (0.25 g, 0.5 mmol) in methanol (5 mL) was added to a slurry of activated zinc in a 1:1 mixture of methanol to water (45 mL). The flask was stirred vigorously under nitrogen for 24 h. The mixture was filtered through a pad of non-acid-washed Celite 545, and the pad was rinsed with methanol (3 × 25 mL). The fractions were combined, condensed, and placed on a column of CHP20P resin. The tetraene ester was eluted with a gradient of methanol in water (20–100%) and treated with 1 N aqueous sodium hydroxide (2 mL). After about 1 h, the reaction mixture was placed on an CHP20P column and the product was eluted with a gradient of methanol in water (20–100%) to afford 65 mg (30%) of the sodium salt, which solidified after concentration. Since coupling constants could not be obtained on the sample in methanol-*d*₄, DMSO-*d*₆ was used: ¹H NMR (DMSO-*d*₆) δ 3.20 (m, 1H), 3.48 (m, 2H), 3.5 (q, *J* = 15.9 Hz, 1H), 3.88 (dq, *J* = 14.8, 4.8 Hz, 2H), 3.97 (m, 1H), 4.42 (m, 1H), 5.28 (d, *J* = 4.9 Hz, 1H), 5.82 (dd, *J* = 14, 5.6 Hz, 1H), 6.00 (m, 3H), 6.32 (m, 2H), 6.55 (br s, 1H), 6.7 (dd, *J* = 14, 9.9 Hz, 1H), 6.85 (dd, *J* = 15, 9.9 Hz, 1H), 6.94 (m, 2H), 7.09 (m, 2H); ¹³C NMR (125 MHz, CD₃OD) δ 72.1, 72.2, 73.9, 74.2, 74.3, 75.3, 117.0, 117.2, 117.5, 117.5, 128.7, 129.5, 130.3, 131.6, 133.0, 133.3, 134.7, 135.4, 136.0, 157.1, 158.3, 160.2, 178.9. Anal. (C₂₁H₂₄FO₇Na·0.8H₂O) C, H, F, Na.

Cutaneous Model of Inflammation. The calcium ionophore induced model of acute inflammation was used as described.¹² Briefly, calcium ionophore A-23187 (10 μL, 0.1% w/v), with or without the anti-inflammatory agent, was applied topically to the dorsal surface of mouse ears, using isopropylmyristate as the vehicle. The animals were euthanized after 24 h. Ear weight was used as an indicator of edema. The extent of granulocyte and neutrophil infiltration was determined on the basis of the measurement of peroxidase and elastase activity, respectively, in mouse ear homogenates.

Air Pouch Model of Inflammation. The mice used in the study were age-matched male Balb/c, 6–8 weeks old [purchased from Sprague-Dawley] and were in groups of 20. On day 0, all mice were anesthetized with 3% isoflurane. Dorsal areas were shaved, cleaned with alcohol swabs, and injected subcutaneously with sterile air (3 mL, passed through 20 μm filter) near the tail. On day 3, all mice were injected with 3 mL of sterile air. On day 6, the air pouches of anesthetized mice were injected sequentially with 900 μL of either **2** or **3** in 0.1% ethanol/PBS or vehicle and with 100 000 units of recombinant mouse TNF-α (0.1 mL PBS; Boehringer Mannheim). Four hours after TNF injection, mice were euthanized with carbon dioxide. Air pouches were lavaged three times with 3 mL of sterile PBS. The cellular exudates were centrifuged for 15 min at 2000 rpm, and the resulting cell pellets were resuspended in 1 mL of sterile PBS/10% BSA. The total number of leukocytes, collected from the pouches, was counted using a Coulter Z1 counter. Total neutrophils were enumerated by differential cell counts on stained slides.

Acknowledgment. The authors thank Eginhard Matzke and Detlef Opitz (Research Business Area Dermatology, Schering AG) and Jerry Dallas (Biophysics, Berlex Biosciences) for excellent technical assistance. We acknowledge the support of Drs. H. Daniel Perez, Khusru Asadullah, and Gary B. Phillips for this work.

References

- Serhan, C. N. Lipoxins and aspirin-triggered 15-epi-lipoxin biosynthesis: an update and role in anti-inflammation and pro-resolution. *Prostaglandins Other Lipid Mediators* **2002**, 68–69, 433–455.
- Serhan, C. N.; Hamberg, M.; Samuelsson, B. Trihydroxytetraenes: a novel series of compounds formed from arachidonic acid in human leukocytes. *Biochem. Biophys. Res. Comm.* **1984**, 118, 943–949.
- Adams, J.; Fitzsimmons, B. J.; Rokach, J. Synthesis of Lipoxins: Total Synthesis of Conjugated Trihydroxy Eicosatetraenoic Acids. *Tetrahedron Lett.* **1984**, 25, 4713–4716.
- Corey, E. J.; Su, W. G. Simple Synthesis and Assignment of Stereochemistry of Lipoxin A. *Tetrahedron Lett.* **1985**, 26, 281–284.
- Nicolaou, K. C.; Webber, S. E. A General Strategy for the Total Synthesis of the Presumed Lipoxin Structures. *J. Chem. Soc., Chem. Commun.* **1985**, 297–298.
- Rodriguez, A. R.; Spur, B. W. Total Synthesis of aspirin-triggered 15-epi-lipoxin A4. *Tetrahedron Lett.* **2001**, 42, 6057–6060.
- Levy, B. D.; Serhan, C. N. Exploring new approaches to the treatment of asthma: potential roles for lipoxins and aspirin-triggered lipid mediators. *Drugs Future* **2003**, 39, 373–384.
- Wallace, J. L.; Fiorucci, S. A Magic Bullet for Mucosal Protection ... and Aspirin Is the Trigger! *Trends Pharmacol. Sci.* **2003**, 24, 323–326.
- Clish, C. B.; Levy, B. D.; Chiang, N.; Tai, H. H.; Serhan, C. N. Oxidoreductases in lipoxin A4 metabolic inactivation: A novel role for 15-oxaprostaglandin 13-reductase/leukotriene B4 12-hydroxydehydrogenase in inflammation. *J. Biol. Chem.* **2000**, 33, 25372–25380.
- Serhan, C. N.; Maddox, J. F.; Petasis, N. A.; Akritopoulou-Zanze, I.; Papayianni, A.; Brady, H. R.; Colgan, S. P.; Madara, J. L. Design of Lipoxin A4 Stable Analogs That Block Transmigration and Adhesion of Human Neutrophils. *Biochemistry* **1995**, 34, 14609–14615.
- Levy, B. D.; De Sanctis, G. T.; Devchand, P. R.; Kim, E.; Ackerman, K.; Schmidt, B. A.; Szczeklik, W.; Drazen, J. M.; Serhan, C. N. Multi-pronged inhibition of airway hyperresponsiveness and inflammation by lipoxin A₄. *Nat. Med.* **2002**, 8, 1018–1023.
- Schottelius, A. J.; Giesen, C.; Asadullah, K.; Fierro, I. M.; Colgan, S. P.; Bauman, J.; Guilford, W. J.; Perez, H. D.; Parkinson, J. F. An aspirin-triggered lipoxin A4 stable analog displays a unique topical anti-inflammatory profile. *J. Immunol.* **2002**, 168, 7064–7070.
- Gewirtz, A. T.; Collier-Hyams, L. S.; Young, A. N.; Kucharzik, T.; Guilford, W. J.; Parkinson, J. F.; Williams, I. R.; Neish, A. S.; Madara, J. L. Lipoxin A4 analogs attenuate induction of intestinal epithelial proinflammatory gene expression and reduce the severity of dextran sodium sulfate-induced colitis. *J. Immunol.* **2002**, 168, 5260–5267.
- Aliberti, J.; Serhan, C. N.; Sher, A. Parasite-induced lipoxin A4 is an endogenous regulator of IL-12 production and immunopathology in *Toxoplasma gondii* infection. *J. Exp. Med.* **2002**, 196, 1253–1262.
- Clish, C. B.; O'Brien, J. A.; Gronert, K.; Stahl, G. L.; Petasis, N. A.; Serhan, C. N. Local and systemic delivery of a stable aspirin-triggered lipoxin prevents neutrophil recruitment in vivo. *Proc. Natl. Acad. Sci. U.S.A.* **1999**, 96, 8247–8252.
- Phillips, E. D.; Chang, H.-F.; Holmquist, C. R.; McCauley, J. P. Synthesis of methyl (5*R*,6*R*,7*E*,9*E*,11*Z*,13*E*,15*S*)-16-(4-fluorophenoxy)-5,6,15-trihydroxy-7,9,11,13-hexadecatetraenoate, an analogue of 15*R*-lipoxin A4. *Bioorg. Med. Chem. Lett.* **2003**, 13, 3223–3226.
- Nicolaou, K. C.; Veale, C. A.; Webber, S. E.; Katerinopoulos, H. Stereocontrolled Total Synthesis of Lipoxins A. *J. Am. Chem. Soc.* **1985**, 107, 7515–7518.
- Robinson, R. S.; Clark, J. S.; Holmes, A. B. The Synthesis of (+)-Laurencin. *J. Am. Chem. Soc.* **1993**, 115, 10400–10401.
- Gooding, O. W.; Beard, C. C.; Cooper, G. F.; Jackson, D. Y. Triply Convergent Synthesis of 15-(Phenoxymethyl) and 4,5-Allenyl Prostaglandins. Preparation of an Individual Isomer of Enprostil. *J. Org. Chem.* **1993**, 58, 3681–3686.
- Hofmeister, H.; Annen, K.; Laurent, H.; Wiechert, R. A Novel Entry to 17α-Bromo- and 17α-Iodoethynyl Steroids. *Angew. Chem., Int. Ed. Engl.* **1984**, 23, 727–729.
- Bohlmann, F.; Rotard, W. Synthese von (2*E*,4*Z*)-2,4,11-Dodecatrien-1-ol, einem Abbauprodukt der Linolensäure (Synthesis of (2*E*,4*Z*)-2,4,11-Dodecatrien-1-ol, a Degradation Product of Linolenic Acid. *Liebigs Ann. Chem.* **1982**, 1216–1219.
- Boland, W.; Schroer, N.; Sieler, C.; Feigel, M. 96. Stereospecific Syntheses and Spectroscopic Properties of Isomeric 2,4,6,8-Undecatetraenes. New Hydrocarbons from the Marine Brown Alga *Giffordia mitchellae* Helv. *Chim. Acta* **1987**, 70, 1025–1040.
- Wheatley, J. R.; Beacham, A. R.; Lilley, P. M. deQ.; Watkin, D. J.; Fleet, G. W. J. Ketals of L-Rhamnoheptanolactones: Potential Mimics of L-Rhamnose. *Tetrahedron: Asymmetry* **1994**, 5, 2523–2534.
- Ellis, C. K.; Smigel, M. D.; Oates, J. A.; Oelz, O.; Sweetman, B. J. Metabolism of prostaglandin D2 in the monkey. *J. Biol. Chem.* **1979**, 254, 4152–4163.
- Sturzebecher, S.; Haberey, M.; Muller, B.; Schillinger, E.; Schroder, G.; Skuballa, W.; Stock, G.; Vorbruggen, H.; Witt, W. Pharmacological profile of a novel carbacyclin derivative with high metabolic stability and oral activity in the rat. *Prostaglandins* **1986**, 31, 95–109.

- (26) Guindon, Y.; Delorme, D.; Lau, C. K.; Zamboni, R. Total Synthesis of LTB₄ and Analogues. *J. Org. Chem.* **1988**, *53*, 267–275.
- (27) Skuballa, W.; Schillinger, E.; Stuerzebecher, C. St.; Vorbrueggen, H. Synthesis of a New Chemically and Metabolically Stable Prostacyclin Analogue with High and Long-Lasting Oral Activity. *J. Med. Chem.* **1986**, *29*, 313–315.
- (28) Takano, T.; Clish, C. B.; Gronert, K.; Petasis, N.; Serhan, C. N. Neutrophil-Mediated Changes in Vascular Permeability Are Inhibited by Topical Application of Aspirin-Triggered 15-Epi-lipoxin A₄ and Novel Lipoxin B₄. *J. Clin. Invest.* **1998**, *101*, 819–826.
- (29) Hachicha, M.; Pouliot, M.; Petasis, N. A.; Serhan, C. N. Lipoxin (LX) A₄ and aspirin-triggered 15-epi-LXA₄ inhibit tumor necrosis factor 1 α -initiated neutrophil responses and trafficking: regulators of a cytokine-chemokine axis. *J. Exp. Med.* **1999**, *189*, 1923–1930.
- (30) Serhan, C. N.; Takano, T.; Clish, C. B.; Gronert, K.; Petasis, N. Aspirin-triggered 15-epi-lipoxin A₄ and novel lipoxin B₄ stable analogues inhibit neutrophil-mediated changes in vascular permeability. *Adv. Exp. Med. Biol.* **1999**, *469*, 287–293.

JM030569L